Spontaneous Injection in Microcolumn Separations

ARTICLE *in* ANALYTICAL CHEMISTRY · AUGUST 1994

Impact Factor: 5.64 · DOI: 10.1021/ac00086a018 · Source: PubMed

5 AUTHORS, INCLUDING:

Richard Zare
Stanford University
1,146 PUBLICATIONS **43,123** CITATIONS

Anal. Chem. 1994, *66*, 2318–2329

Spontaneous Injection in Microcolumn Separations

Harvey A. Fishman, Nabeel M. Amudi, Thomas T. Lee,† Richard H. Scheller,‡ and Richard N. Zare*

Department of Chemistry, Stanford University, Stanford, California 94305

The phenomenon of spontaneous (ubiquitous) injection in microcolumn separations has been characterized to improve quantitative precision for ultramicrosampling and to enhance separation efficiency. By combining fluorescence imaging, video microscopy, and measurements from capillary electrophoresis, we demonstrate that spontaneous injection is caused primarily by an interfacial pressure difference formed at the inlet of the capillary. This complex injection mechanism has been modeled with some simple assumptions based on fluid dynamics. In particular, studies showed that extraneous injection is reduced up to 12-fold by etching the capillary inlet or by using a thin-walled capillary. Variations by a factor of 2 in the injection length can result from delays between sample introduction and reinsertion into the inlet vial if the timing is not controlled precisely. Evidence is presented that evaporation of buffer from the inlet can reduce the injection length by more than 1 order of magnitude.

Microchannel separation techniques, such as capillary electrophoresis (CE) and open tubular liquid chromatography, are especialy well-suited for chemical analysis in small volumes.[1] The ability to perform subnanoliter injections[1-3] offers many opportunities for chemically profiling complex samples in cellular biochemistry and biotechnology. Examples include the analysis of single cells, subcellular organelles, and vesicles.[1-8] The use of narrow injection plugs also significantly improves separation efficiency and resolution.[9-11] Indeed, the importance of performing small injections has been recognized, and several approaches for ultramicrosample injection and manipulation have been demonstrated including CE on a chip,[12,13] electrophoresis across a gap,[14,15] specialized microinjection techniques,[16-19] and on-column microreactions.[20,21]

Simply touching the capillary to the sample solution, however, has long been recognized to cause an extraneous injection that accounts for the nonzero intercept when calibrating injection volumes in CE[9-11,22,23] and in electrokinetic chromatography.[24] As sample volumes decrease further, reducing this type of injection error becomes critical. Even for routine analysis, capillary electrophoresis has suffered from poor reproducibility,[25-28] and improvements in quantitative precision and accuracy are needed. Grushka and McCormick[9] were the first to report on this extraneous injection, a phenomenon they called "ubiquitous injection". They found that ubiquitous injection could start as soon as the capillary made contact with the sample. After the capillary was removed, the sample had penetrated ~700 μm into the capillary, corresponding to an approximate volume of 3 nL for a 75-μm-i.d. capillary. Furthermore, they reported that the process of sample penetration showed no correlation to the interval of time the capillary was in contact with the sample. Other studies[27,29] established that this extraneous injection would lead to errors in calibration and quantitation for which compensation is difficult even with internal standards. In addition to degrading quantitation, this extraneous injection can severely reduce separation efficiency.[9-11]

Dose and Guiochon[27,29] discussed an inherent difficulty in quantitative CE injections, namely, that the injection zone boundaries are defined by interfaces between miscible solutions that spontaneously lead to dispersion. They argued that diffusion might play the dominant role in extraneous injection. Using computer simulations, they showed that the concentration gradient at the inlet caused a rapid net flow of the sample into or out of the capillary. In addition, as a filled capillary touches a liquid surface, the surface tension is broken and the resultant convective mixing can contribute to extraneous injection of the sample.[30] Although these arguments based

† Current Address: Gilead Sciences, Foster City, CA 94404.
‡ Howard Hughes Medical Institute, Department of Molecular and Cellular Physiology, Stanford University, Stanford, CA 94305.

(1) Kennedy, R. T.; Oates, M. D.; Cooper, B. R.; Nickerson, B.; Jorgenson, J. W. *Science* **1989**, *246*, 57–63.
(2) Olefirowicz, T. M.; Ewing, A. G. *Anal. Chem.* **1990**, *62*, 1872–1876.
(3) Ewing, A. G.; Wallingford, R. A.; Olefirowicz, T. M. *Anal. Chem.* **1989**, *61*, 292A–303A.
(4) Lee, T. T.; Yeung, E. S. *Anal. Chem.* **1992**, *64*, 3045–3051.
(5) Hogan, B.; Yeung, E. S. *Anal. Chem.* **1992**, *64*, 2841–2845.
(6) Cooper, B. R.; Jankowski, J. A.; Leszczyszyn, D. J.; Wightman, R. M.; Jorgenson, J. W. *Anal. Chem.* **1992**, *64*, 691–694.
(7) Sweedler, J. V.; Shear, J. B.; Fishman, H. A.; Zare, R. N.; Scheller, R. H. *Proc. SPIE-Int. Soc. Opt. Eng.* **1992**, *1439*, 27–33.
(8) Sweedler, J. V.; Fuller, R.; Tracht, S.; Timperman, A.; Toma, V.; Khatib, K. *J. Microcolumn Sep.* **1993**, *5*, 403–412.
(9) Grushka, E. M.; McCormick, R. M. *J. Chromatogr.* **1989**, *471*, 421–428.
(10) Huang, X.; Coleman, W. F.; Zare, R. N. *J. Chromatogr.* **1989**, *480*, 95–110.
(11) Schwartz, H. E.; Melera, M.; Brownlee, R. G. *J. Chromatogr.* **1989**, *480*, 129–139.
(12) Harrison, D. J.; Fluri, K.; Seiler, K.; Fan, Z.; Effenhauser, C. S.; Manz, A. *Science* **1993**, *261*, 895–897.
(13) Effenhauser, C. S. Manz, A.; Widmer, H. M. *Anal. Chem.* **1993**, *65*, 2637–2642.
(14) Kuhr, W. G.; Licklider, L.; Amankwa, L. *Anal. Chem.* **1993**, *65*, 277–282.
(15) Amankwa, L.; Kuhr, W. G. *Anal. Chem.* **1993**, *65*, 2693–2697.
(16) Linhares, M. C.; Kissinger, P. T. *Anal. Chem.* **1991**, *63*, 2076–2078.
(17) Kennedy, R. T.; Jorgenson, J. W. *Anal. Chem.* **1988**, *60*, 1521–1524.
(18) Wallingford, R. A.; Ewing, A. G. *Anal. Chem.* **1988**, *60*, 1972–1975.
(19) Wallingford, R. A.; Ewing, A. G. *Anal. Chem.* **1987**, *59*, 678–681.
(20) Fishman, H. A.; Shear, J. B.; Sweedler, J. V.; Zare, R. N.; Scheller, R. H. The Pittsburgh Conference on Analytical Chemistry and Applied Spectroscopy, March 9–12, New Orleans, LA, 1992; Abstract 300.
(21) Harmon, B. J.; Patterson, D. H.; Regnier, F. E. *Anal. Chem.* **1993**, *65*, 2655–2662.
(22) Rose, D. J., Jr.; Jorgenson, J. W. *Anal. Chem.* **1988**, *60*, 642–648.
(23) Honda, S.; Iwase, S.; Fujiwara, S. *J. Chromatogr.* **1987**, *404*, 313–320.
(24) Bruin, G. J. M.; Tock, P. P. H.; Kraak, J. C.; Poppe, H. *J. Chromatogr.* **1990**, *517*, 557–572.
(25) Li, S. F. Y. *Capillary Electrophoresis*; Elsevier: London, 1992.
(26) Weinberger, R. *Practical Capillary Electrophoresis*; Academic Press: Boston, MA, 1993.
(27) Dose, E. V.; Guiochon, G. *Anal. Chem.* **1992**, *64*, 123–128.
(28) Lookabaugh, M.; Biswas, M.; Krull, I. S. *J. Chromatogr.* **1991**, *549*, 357–366.
(29) Dose, E. V.; Guiochon, G. *Anal. Chem.* **1991**, *63*, 1063–1072.
(30) Bird, R. B.; Stewart, W. E.; Lightfoot, E. N. *Transport Phenomena*; Wiley: New York, 1960.

0003-2700/94/0366-2318$04.50/0

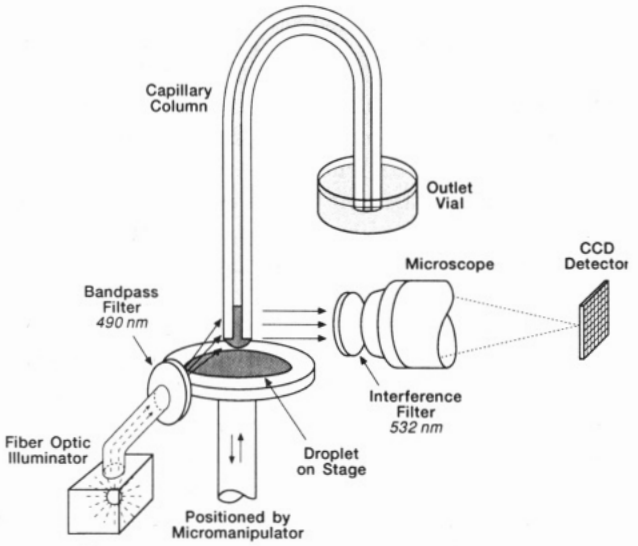

Figure 1. Fluorescence imaging system used to visualize and quantitate directly spontaneous extraneous injection. A video-speed CCD camera was reversibly interchanged with a low-noise, scientific-grade CCD camera. Objects are not drawn to scale. A 10-μL drop was injected onto the stage for all experiments.

on diffusion and convection can partially explain how sample enters the capillary, additional factors must contribute to account for the observed amount and speed of injection.[9-11,23,24] Several additional explanations have been offered, but the dominant mechanism responsible for this spontaneous (ubiquitous) injection remains unresolved and a matter of some concern to the CE research community.

In this work, we characterize a predominant mechanism of spontaneous extraneous injection in capillary electrophoresis. Using a fluorescence imaging system equipped with a scientific-grade charge-coupled device (CCD), video microscopy, and quantitative measurements from capillary electrophoresis, we demonstrate that extraneous injection originates primarily from the formation of an interfacial pressure difference across a droplet at the inlet of the capillary upon removal from the sample reservoir. Sample is introduced into the capillary by a process known in the chemical engineering community as *spontaneous fluid displacement*.[31] Because penetration is time dependent, transfer times that differ between sample introduction and reinsertion into the inlet vial can result in reproducibility errors. In addition, we also identify that the vapor pressure surrounding the capillary during the transfer delay may significantly affect the injection process and lead to a massive loss of running buffer, which causes sample compression in the entrance of the column. We demonstrate the deleterious nature of both spontaneous fluid displacement and sample compression to injections in capillary electrophoresis and offer practical methods for controlling these effects.

EXPERIMENTAL SECTION

Imaging System. Figure 1 shows the imaging system used to visualize and quantitate extraneous injection plugs. The inlet end of a fused silica capillary column (25 × 348, 50 × 345, 75-μm i.d. × 345-μm o.d.) (Polymicro Technologies, Phoenix, AZ) was cleaved by first scoring the polyimide coating with a ceramic cleaving square (Polymicro Technologies) and then carefully bending the capillary to fracture it. With care, this procedure consistently produced a nearly flat surface (as observed under a stereomicroscope) with an angle of ~87 ± 3° with respect to the capillary wall. A 5-mm section of the polyimide coating at the inlet end was removed with a Bunsen burner flame. The capillary was then fixed in position and imaged by a stereomicroscope (SMZ-2T, Nikon, Tokyo, Japan). For the qualitative visualization experiments, images were taken with a CCD video camera (Sony) and recorded with a VHS video recorder (Panasonic). A fiber-optic bundle (Cole-Palmer, Niles, IL) was directed into the microscope's built-in optics to provide Koehlerlike illumination. For displaying images on film, the video recorder was stopped (paused) and photographs were taken of the video screen (Sony Trinitron) using a Nikon 35-mm camera (Model N80085).

For the fluorescence imaging studies, a liquid-nitrogen-cooled (−126 °C), scientific-grade CCD camera (Photometrics, Tucson, AZ) equipped with a 512 × 512 CCD chip (PM512, Photometrics) was used for imaging. The CCD was controlled by IPLab software (Signal Analytics, Vienna, VA) using a photometrics NU-200 camera controller board, CC200 camera controller, and PS200 power supply module. The fiber-optic bundle directly illuminated the capillary with broad-band excitation that was sent through a 490-nm bandpass filter (BG-7, Schott Glass Technologies, Duryea, PA). Fluorescence from the capillary was collected from the microscope optics (32× magnification), which had a 532-nm interference filter (Oriel, Stratford, CT) mounted on its front. The CCD was positioned at the focal plane of the stereomicroscope. A chamber was built around a small platform that holds the sample solution. The chamber was made from a standard plastic cuvette (1-cm path length) that was inverted and the open end sealed to a piece of Plexiglas. A small hole (slightly larger than the capillary) was drilled into the top of the chamber so that the capillary could enter for the purpose of making injections.

Sample solution was injected onto the small platform inside the chamber. For experiments performed in a saturated environment, the chamber was filled with water to the level of the platform to provide a water-vapor-saturated environment. For experiments performed in ambient conditions, an identical chamber was made with the top completely open to the atmosphere, and the humidity of the air in the chamber (Palo Alto, CA) ranged from ~40 to 65%. Each chamber was mounted on a Plexiglas plank raised and lowered by a micromanipulator (Prior, England). To prevent inadvertent hydrodynamic injection, each capillary was positioned so that the meniscus in the outlet reservoir would be 2–3 mm above the meniscus of the sample solution. Moreover, the capillary was in contact with the sample no longer than 5 s.

CCD Image Processing. CCD images were collected by a Macintosh IIci computer using the IPLab spectrum software. The capillary inlet was imaged onto a region of the CCD that had a width ranging from 20 to 60 (2 × 2 binned pixels) and a length from 200 to 400 (2 × 2 pixels). Because the magnification was slightly different for each capillary inner diameter, the pixel geometry read out by the CCD varied to accommodate the different image dimensions. These pixel

(31) Marmur, A. In *Modern Approaches to Wettability: Theory and Applications*; Schrader, M. E., Loeb, G., Eds.; Plenum: New York, 1992; pp 327–356.

geometries were read out with exposure times between 0.1 and 0.5 s and a gain setting of 1.0. Collection rates were between 0.75 and 1.7 Hz for entire snapshots. Image dimensions were estimated by using the known premeasured outer diameter of the capillary as an internal calibration. Images of the capillaries had similar cross-sectional profiles. From these images we could estimate the position of the edge of the outer capillary wall with an uncertainty of 3 pixels, thus making the internal calibration distances accurate to within 6 pixels (final injection lengths ranged between 50 and 165 pixels). The front end of the capillary was identified by a bright spot that appeared at the front end of all capillaries before and after the fluorescein solution entered the column. The fluorescence response from the channel of the capillary filled with a homogeneous solution of fluorescein was roughly uniform and varied linearly with the concentrations used in these studies.

To determine spontaneous extraneous injection lengths, a plot of the fluorescence intensity along the length of the capillary channel was obtained. First, pixels across the width of the channel were averaged. This averaging resulted in a single intensity value for each point along the length of the column, thus resulting in a one-dimensional image slice down the capillary. These slices were converted to one-dimensional text file arrays and then analyzed on the Macintosh IIci using programs written in Igor (WaveMetrics, Lake Oswego, OR). Plots of the image slice showed the concentration profile along the length of the injection plug. The front end of the concentration profile for an injection plug is defined by an error function.[32,33] To quantitate the length of the injection, the front end of the injection profile was defined as the point where the intensity had decreased by 50% of the maximum (the inflection point). The maximum intensity level was determined by taking the average intensity along a segment of the uniformly filled portion of the capillary, just prior to the injection front. For all curves, the 50% point compared favorably with the actual calculated inflection point and was used because it was easier to obtain. By use of the 50% point for the leading edge, injection lengths were normalized for each image. Thus, comparisons between the kinetics of injection penetration for each run with a particular capillary inner diameter were internally consistent and averaged out any nonuniformity in illumination or fluorescence intensity. For these reasons, flat-field correction of the data was not performed. Although no dark-current subtractions on the CCD images were made, baseline subtractions were carried out on the intensity profiles along the column length. To more easily compare the amount of injection for different capillary inner diameters, the length of the injection plug was converted to an effective cylinder with a given volume. Calculation of the volume in this manner with the assumption of a homogenous solution provided a reasonable estimate of the amount of sample. The penetration kinetics are obtained by plotting this effective volume against time. For these penetration curves, we have chosen the time point immediately before a sharp increase in penetration kinetics as the starting time for spontaneous injection.

CE Detection System. Separations were performed using a home-built CE system with an absorbance detector (Isco CV4, RI). The detector wavelength was set at 340 nm with a time contant of 0.2 s. The voltage control has been described elsewhere.[34] The inlet of the capillary was manually transferred from the sample solution to the inlet reservoir. As in the CCD imaging studies, injections were made from a 10-μL droplet on a patform surrounded by the cuvette chamber. A larger hole in the top of the chamber was used to facilitate the manual transfers. In addition to filling the chamber to the level of the platform with water, a saturated environment for the CE experiments was ensured by positioning the capillary just above the sample droplet after solution breakup. The capillary was in contact with the sample no longer than 5 s. Timing for the transfer was accomplished using either a stopwatch or an alarm timer. During the injection, the sample solution was held 1–2 mm below the level of the outlet reservoir to prevent inadvertent hydrodynamic injection. Similarly, to prevent loss of the sample from inadvertent hydrodynamic outflow when the capillary was reinserted into the inlet buffer reservoir, the outlet reservoir was held 1–2 mm below the inlet. A delay of ~10 s occurred between reinserting the capillary into the inlet vial and applying the voltage across the capillary. Data were collected with a 486 computer (Adisys, Santa Clara, CA) using Lab Calc data acquisition software and a Chrom-1AT data acquisition board (Galactics, NH). Peak areas were determined using the Lab Calc software algorithm. Analyte bands that travel past the detector at different velocities give different peak areas. Hence, only analyte bands that had migration times within 5% of each other were used in this analysis. Random noise spikes in electropherograms were removed for clarity of presentation.

Chemicals and Reagents. All solutions were repared from a Millipore water filter system (Milli-Q Plus/UV, Milli-RO 6 Plus, Waters, Bedford, MA). A 15 mM phosphate buffer, pH 8.9 (Mallinckrodt, San Francisco, CA), was used for all studies. For CE runs, the buffer was filtered through 0.2-μm pore size syringe filters. Imaging studies were carried out using a 0.4 mM 2′,7′-dichlorofluorescein solution dissolved in 15 mM, pH 8.9 phosphate buffer. Stock solutions of N_ϵ-dansyl-L-lysine, N_α-dansyl-L-tryptophan, and dansyl-L-alanine (Sigma Chemical Co., St. Louis, MO) prepared in the phosphate running buffer were stored in the refrigerator and serially diluted as needed before use.

Capillary Treatments. All capillaries were conditioned with 0.1 M sodium hydroxide (Mallinckrodt) prior to use, and buffer was then electrophoresed through the column for 1 h. For some studies, the outer surface of the capillary was silanized by holding an air-filled column in a solution of dimethyldichlorosilane in toluene (silanization solution from Supelco, Bellefonte, PA) for 30 min. Afterward, the column was purged with nitrogen and air-dried for several minutes. The outer diameter of some capillaries was chemically etched with 0.1 M hydrofluoric acid (Sigma) for 2.5 h. Because hydrofluoric acid is extremely harmful upon skin contact, thick gloves and protective clothing must be worn when it is handled, and the vapors must not be inhaled. To maintain a constant inside diameter, the other end of the column was

(32) Crank, J. *The Mathematics of Diffusion*; Clarendon Press: Oxford, UK, 1956.
(33) Giddings, J. C. *Unified Separation Science*; Wiley: New York, 1991.
(34) Sweedler, J. V.; Shear, J. B.; Fishman, H. A.; Zare, R. N.; Scheller, R. H. *Anal. Chem.* **1991**, *63*, 496–502.

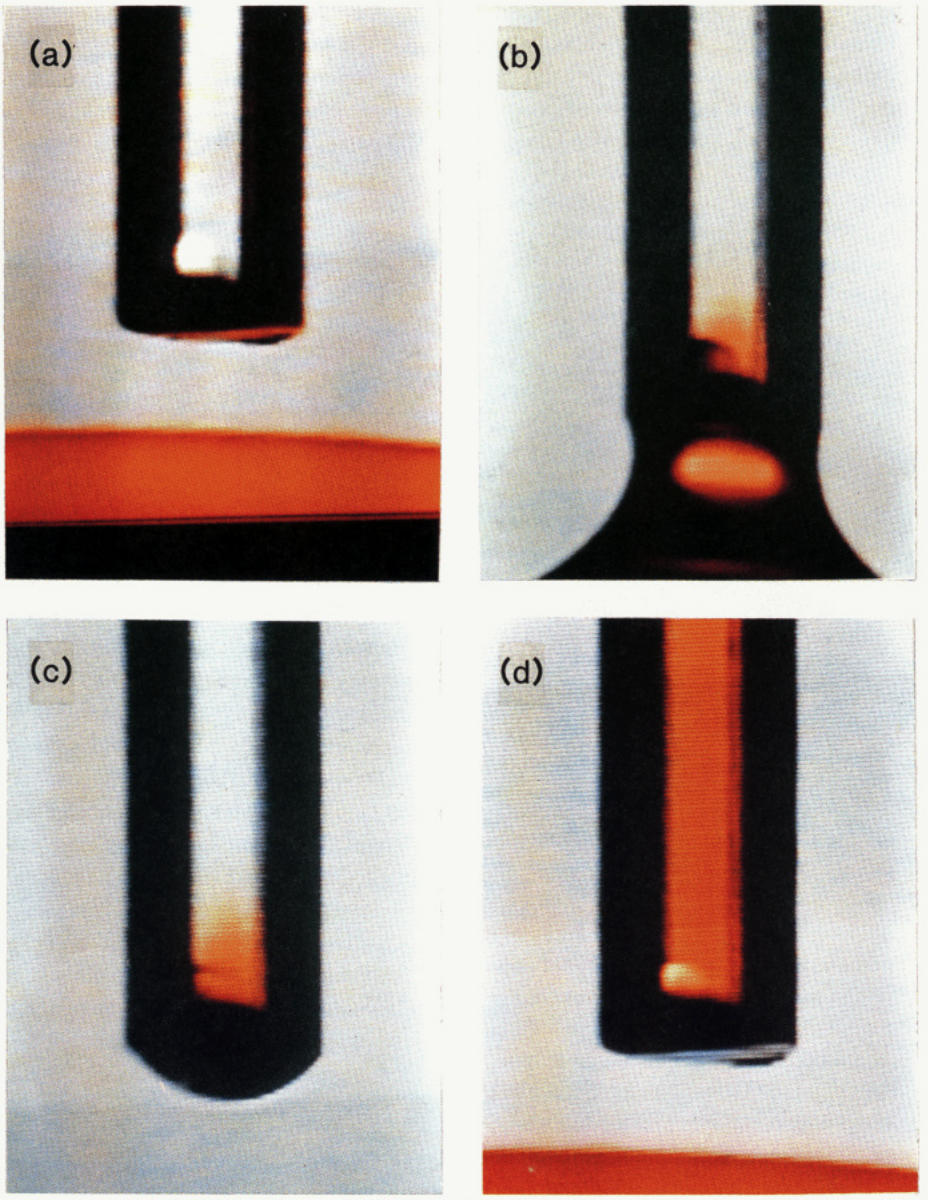

Figure 2. Video images showing the inlet end of a 75-μm-i.d., 343-μm-o.d. capillary with polyimide removed. Capillary (a) prior to sample contact, (b) contact with the sample immediately before solution breakage, (c) 34 ms after leaving solution, and (d) ~10 s after leaving solution. The orange solution below the capillary inlet is 2′,7′-dichlorofluorescein dissolved in 15 mM, pH 8.9 phosphate buffer.

attached to a pressure-regulated nitrogen tank, thereby creating a constant flow of nitrogen through the column to prevent the acid from entering the inside of the column. The capillary was rinsed with water before use.

To maintain uniform wetting on the outside surface of the capillary (i.e., to reproduce the surface conditions), excess water droplets were removed from the outside of the capillary before each run. For the CCD imaging experiments, this removal was accomplished by slowly withdrawing the analyte solution from contact with the capillary. For CE runs, water drops that adhered to the outside capillary surface were removed by lightly drawing the edge of a cover slip across the surface. Only runs with no noticeable surface spreading after sample contact were used in these studies.

THEORY

A video microscope imaging system reveals an unexpected mechanism for spontaneous extraneous injection. Parts a–d of Figure 2 show images of the inlet of a fused silica capillary (75-μm i.d., 343-μm o.d.) as it enters and leaves a solution of fluorescein dissolved in the running buffer. Upon contact with the surface (Figure 2b), the solution immediately wets the sides of the capillary and spreads upward until the interfacial energy between the water and the glass are balanced.[35] As the solution is slowly lowered below the capillary inlet, the solution forms a quasicylinder of liquid that eventually becomes unstable toward the necking (Rayleigh instability[36,37] and collapses into two segments. One segment of the collapsed cylinder forms a droplet that adheres to the end of the capillary (Figure 2c), and the rest falls back into the bulk of the solution. Spontaneously, the droplet penetrates into the capillary, and within a few seconds, the entire droplet

(35) Hunter, R. J. *Foundations of Colloid Science*; Clarendon Press: Oxford, UK, 1987; Vol. 1, pp 272–299.
(36) Rayleigh, Lord. *Proc. London Math. Soc.* **1878**, *10*, 4–13.
(37) Rumscheidt, F. D.; Mason, S. G. *J. Colloid Interface Sci.* **1962**, *17*, 260–269.

has entered into the capillary and displaced the buffer present (Figure 2d). This type of capillary penetration from a limited reservoir has been termed *spontaneous liquid–liquid displacement* or *spontaneous fluid displacement* by Marmur.[31]

Interfacial pressure difference across the curved droplet drives the penetration process. As originally noted by Young[38] and Laplace[39] around the turn of the 19th century, the pressure difference, Δp, across a curved surface is given by the following:

$$\Delta p = \gamma\left(\frac{1}{R_1} + \frac{1}{R_2}\right) \tag{1}$$

where γ is the surface tension of the solution and R_1 and R_2 are the principal radii of curvature of the droplet. If the meniscus is approximated by a hemispherical surface, then the pressure difference becomes

$$\Delta p = 2\gamma/R \tag{2}$$

The droplet maintains the curved shape to minimize the surface area.[40] As long as an inward pressure exists at the entrance of the capillary, penetration occurs. The equilibrium condition is one in which a counteracting pressure opposes the interfacial pressure difference from the curvature of the droplet;[31,41–43] in the case of CE, this counterpressure can arise from a height difference between the inlet and outlet reservoirs, so that we have

$$2\gamma/R + \rho g h = 0 \tag{3}$$

where ρ is the density of the solution, g is the gravitational acceleration, and h is the height difference between the reservoirs. From Marmur's results,[31,43] we can predict (and later will show) that the force from the interfacial driving pressure can be much greater than that formed from typical height differences between reservoirs. This pressure may have interesting ramifications for injections in small-bore capillaries (2 and 5 μm).

Flow kinetics for capillary penetration have been described in detail by several authors.[44–46] Lucas[44] and Washburn[45] first developed a quasi-steady-state theoretical approach for capillary penetration that was based on fully developed laminar flow of a Newtonian liquid with negligible inertia effects. They combined the pressure difference across the curved interface with known flow dynamics in a capillary. The total fluid flux of the solution in a capillary is given by the Hagen–Poiseuille equation:[33]

$$\frac{dV}{dt} = \frac{\pi \Delta p r^4}{8 \eta L} \tag{4}$$

where dV/dt is the flux (volume per unit time), Δp is the pressure difference, r is the radius of the inside of the capillary, L is the length of the capillary, and η is the viscosity of the solution. By substituting eq 3 into eq 4, a differential equation for the flow kinetics into a capillary caused by a pressure difference across the droplet is obtained:

$$\frac{2\gamma}{R} - \rho g h - \frac{dV}{dt}\frac{8\eta L}{\pi r^4} = 0 \tag{5}$$

This equation is essentially identical to the general form of the Lucas–Washburn equation[44,45] that describes the kinetics of flow in a capillary in which the pressure difference results from the curved meniscus in classic capillary rise experiments.

Equation 5 allows us to make some general predictions about what types of flow kinetics occur provided we know how the curvature of the meniscus varies in time. In one possible mechanism, the droplet surface can be thought of as a portion of a sphere with the ends attached to the outside of a thin-walled capillary. As the fluid is forced into the capillary, the droplet surface flattens, and accordingly, the radius of curvature of the droplet increases. As the radius of curvature increases, the interfacial pressure difference decreases, and the flow velocity slows down until the droplet penetrates into the capillary. Marmur[31] describes a different geometric situation, in which the droplet is attached at the inner capillary walls, and instead of flattening, it reduces its volume by forming smaller and smaller spheres. This scenario creates an opposite dynamics of flow, namely, one in which the radius of curvature continually decreases, thus leading to greater pressure differences and an increasing penetration velocity. Equation 5 assumes that the droplet is a portion of a sphere that maintains a fixed point of attachment at the outer edge of the capillary. With thin-walled capillaries, the droplet can easily maintain a fixed attachment site; there is a limited amount of surface area on the front annular surface at the capillary inlet to which the droplet can adhere.

In practice, many factors can modify the interfacial energy of the curved meniscus and must be taken into account when the actual interfacial pressure difference at the capillary entrance is modeled. The surface morphology, especially how well the capillary is cleaved, and the wettability of the capillary surface are extremely important. Cohen and Grushka[47] have studied the influence of the shape of the inlet on the observed efficiencies in capillary separations, and they found that straight-edge capillaries are superior to slanted ones. Surface roughness can cause contact angle hysteresis[31] and result in deviations from a spherical droplet surface. In general, any factor that affects the apparent contact angle between the droplet and the capillary surface or the point of attachment can significantly affect the shape and amount of the droplet present at the entrance. With 360-μm-o.d. capillaries, the annular front surface area is significant. Video observations demonstrate that the droplet attaches at the outer edge of the annulus immediately after solution breakage. As the droplet

(38) Young, T. *Philos. Trans. R. Soc. London* **1805**, *95*, 65–87.
(39) Laplace, P. S. de M.; *Supplement au dixieme livre du traite de mecanique celeste*; 1806; Bowditch, N. Translated and annotated; Boston, 1829–1839, 4 vols. Reprinted, Chelsea: New York, 1966.
(40) Adamson, A. W. *Physical Chemistry of Surfaces*, 5th Ed.; Wiley: New York, 1990.
(41) Marmur, A. *J. Colloid Interface Sci.* **1988**, *122*, 209–219.
(42) Marmur, A. *J. Colloid Interface Sci.* **1989**, *130*, 288–289.
(43) Marmur, A. *Chem. Eng. Sci.* **1989**, *44*, 1511–1517.
(44) Lucas, R. *Kolloid Z.* **1918**, *23*, 15–22.
(45) Washburn, E. W. *Phys. Rev.* **1921**, *17*, 273–283.
(46) Szekely, J.; Neumann, A. W.; Chuang, Y. K. *J. Colloid Interface Sci.* **1971**, *35*, 273–278.
(47) Cohen, N.; Grushka, E. *J. Chromatogr.*, in preparation.

penetrates into the capillary, the contact line for the droplet may move toward the inner walls and affect the interfacial pressure difference. In addition, any surface spreading onto the outside walls of the capillary would act to increase the radius of curvature of the meniscus and relax the interfacial energies. For example, when a capillary is cleaved with the front surface edge more rounded and less defined, solution may more easily spread along the outside surface.

Differences in the process where the solution necks and breaks apart to form the droplet at the end of the capillary may also contribute to variability in amount injected.[48] One factor that may affect the breakup of the necking solution and hence the amount of droplet formed on the end is the radius of curvature of the sample solution into which the capillary is inserted. Moreover, the speed at which the capillary leaves the sample solution may affect how much liquid forms at the entrance. For rapid removal, we observed that the droplet formation is not localized to just the front surface of the capillary but instead pours over the edge and spreads along the outside surface of the capillary.

RESULTS AND DISCUSSION

Generality of Mechanism. We tested several different experimental conditions to confirm the generality of this mechanism for spontaneous injection. This penetration process occurred with 75-, 50-, and 25-μm-i.d. capillaries (~345-μm o.d.) with and without the polyimide coating removed. These video experiments were performed with the fluorescein solution dissolved in the same buffer as in the filled column. Qualitatively, we found the same mechanism of injection for the case in which the fluorescein was dissolved in different buffers and at different pHs (pH 8.7 phosphate, pH 9.3 borate, and pH 12 phosphate buffers). Furthermore, the spontaneous injection effect was found to occur with other dyes (bromophenol blue and rhodamine). In 50 trial experiments, we observed that the amount of fluorescein injected simply upon contact with the solution comprised only a small fraction (less than 10%) of the overall amount injected after the capillary was removed entirely from the sample. This reproducible observation is inconsistent with initial reports by Grushka and McCormick,[9] who observed that the sample could penetrate as much as 700 μm upon contact. Spontaneous injection resulted when the capillary was removed from both a small sample reservoir (10-μL droplet on a slide) having a small radius of curvature and from a large sample reservoir (1-mL vial) having a large radius of curvature.

For the capillaries we studied, spontaneous fluid displacement of the droplet was the dominant contribution to extraneous injection. Because many factors can affect the spontaneous injection, we have chosen to study the behavior using a set of capillary conditions that were reproducible in surface flatness, surface wettability, removal speed, and size of the sample solution reservoir (see Experimental Section). Even with some differences in cleave angle and surface roughness (as observed under the microscope), the obtained conditions are sufficiently reproducible to give similar injection amounts (within approximately 10–20%) with different capillary cuts. Although variations in surface conditions from capillary to capillary or differences in the radius of curvature of the sample solution may affect injection amounts, the mechanism of spontaneous fluid displacement is general enough that important trends and conclusions can be derived from investigating more quantitatively a single set of reproducible conditions such as those chosen in this work.

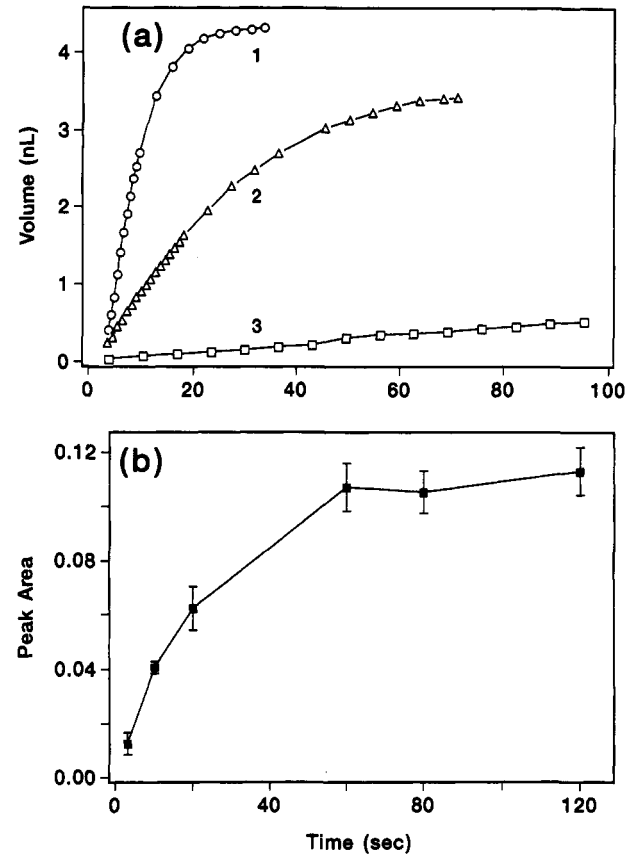

Figure 3. (a) Kinetic curves for spontaneous capillary penetration. The capillary is surrounded by a vapor-saturated environment. Each curve shows the volume of the injection plug as a function of time. Injection plugs were quantitated directly from images taken by a scientific-grade CCD camera. Shown are penetration curves for (1) 75-μm-i.d., 343-μm-o.d. capillary; (2) 50-μm-i.d., 345-μm-o.d. capillary; and (3) 25-μm-i.d., 348-μm-o.d. capillary. Statistics for the injection length after leveling off (mean ±1σ): 132 ± 2.6 pixels (n = 3), 7.4 μm/pixel (75-μm-i.d. capillary); 165 ± 5 pixels (n = 3), 9.9 μm/pixel (50-μm-i.d. capillary); 132 ± 3.5 pixels (n = 2), 13.9 μm/pixel (25-μm-i.d. capillary). The sample consisted of 0.4 mM 2′,7′-dichlorofluorescein dissolved in 15 mM pH 8.9 phosphate buffer; the column length was ~58 cm for each case and was filled with 15 mM, pH 8.9 phosphate buffer. (b) Peak area for dansylated lysine as a function of transfer time. (Analysis is from electropherograms of spontaneous injection of a mixture of the three dansylated amino acids described in Figure 4.) Capillaries were surrounded by a vapor-saturated atmosphere during the transfer. Each point represents the mean peak area for a particular transfer time. Error bars represent 1σ (n = 3).

Penetration Kinetics in Saturated Atmosphere. The kinetics of sample penetration into the capillary were quantitatively imaged using a charge-coupled device. To decouple the effects of evaporation on the droplet, the inlet was contained in a water-vapor-saturated compartment. Shown in Figure 3a are curves quantifying the effective volume of the spontaneous injection as a function of time *after* removal the capillary from the sample solution. Representative penetration curves for 75-, 50-, and 25-μm-i.d., ~345-μm-o.d. capillaries are plotted. As predicted by eq 5, the velocities decreased with

(48) Fishman, H. A.; Scheller, R. H.; Zare, R. N., submitted to *J. Chromatogr.* symposium volume for the 6th International Symposium on High Performance Capillary Electrophoresis.

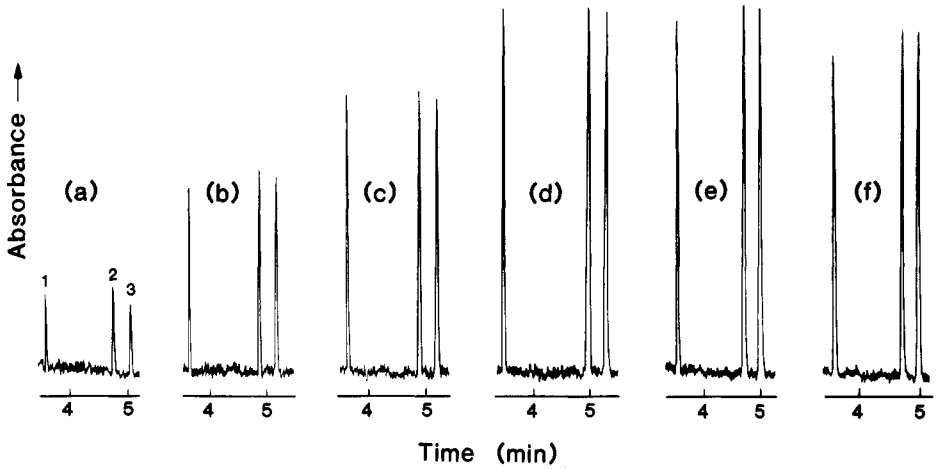

Figure 4. Effect of varying the time between transferring the capillary inlet from the sample solution and reinserting it in the inlet reservoir. The capillary was transferred in a vapor-saturated atmosphere. Each electropherogram shows a separation of ~0.5 mM (1) dansyllysine, (2) dansyltryptophan, and (3) dansylalanine. The different electropherograms correspond to the following transfer times: (a) 2, (b) 10, (c) 20, (d) 60, (e) 80, and (f) 120 s. The mean and standard deviations for each set of delay times are shown in Figure 3b. Separation capillary, 75 μm i.d. × 62 cm (27 cm to detector); buffer, 15 mM phosphate, pH 8.9; 16kV voltage.

smaller inner diameter and the penetration velocity eventually leveled off; this result is consistent with the increasing radius of curvature as the droplet flattens and goes into the capillary. We numerically evaluated eq 5 and compared these numerically predicted penetration curves (not shown) with the penetration curves from the CCD imaging. Although qualitatively similar, the simulated curves exhibited faster penetration kinetics than the experimental findings; this discrepancy suggested that interfacial energy was dissipated under our experimental conditions. According to the measurements obtained by the CCD for the 75-μm-i.d. capillary, the length injected approached 1 mm, an amount that corresponds to a volume of roughly 4 nL of injected material. This amount of material can represent almost half of typical injections in CE. Moreover, these penetration curves show that penetration can be a problem even with smaller capillaries, but the kinetics are markedly slower. This finding suggests that diffusional or convective mixing contributions to spontaneous extraneous injection may become more important as the transfer time and capillary inner diameter decreases. For longer delay times, however, penetration clearly dominates extraneous injection by diffusion or convective mixing.

The ability to form images of the injection kinetics with the CCD and video microscopy provides valuable information about what occurs before the separation voltage is applied. Direct measurements of the peaks resulting from spontaneous injection in actual capillary electrophoresis separations are crucial, however. By recognizing that extraneous injection results from spontaneous fluid displacement, a time-dependent process, the idea becomes apparent that differential delay time *after* withdrawing the capillary from the sample and reinserting it into the inlet solution can substantially affect the amount of the sample droplet that penetrates into the capillary. Figure 3b illustrates the effect of differential delay time on peak area. Each point is the average peak area from a separation of dansylated lysine resulting from a different transfer time, and the error bars represent one standard deviation. The curve shown is for a 50-μm-i.d., 345-μm-o.d. capillary and is qualitatively similar to the shape of the penetration kinetics as determined by CCD imaging.

Figure 4 shows a sequence of electropherograms of three dansylated amino acids. Each group of three peaks results from a single spontaneous extraneous injection. The only difference between them is the length of time between transferring the capillary inlet out of the sample solution and reinserting it into the buffer reservoir. Figure 4 demonstrates that varying the delay time can significantly affect the resulting spontaneous injection peak. The separation shown for each time delay is a representative run of the mean peak area for several identical injections. Mechanistically, once the capillary enters the solution, a curved meniscus no longer gives rise to a spontaneous penetration from a pressure difference; any remaining sample at the entrance will have either diffused away or become washed away by the movement of the capillary through the inlet buffer. The main result from Figures 3 and 4 is that, by inadvertently changing the delay interval, the injection contribution from spontaneous fluid displacement can change by more than 1 order of magnitude.

The amount of injection upon contact with the sample is controlled by diffusion[27] and convection[30] and other possible reported mechanisms that can result in the mixing of the sample with the buffer.[40,48] In the experiments with the 75-μm-i.d. capillaries, less than 10% of the entire possible ubiquitous injection occurs before the capillary is removed from the sample solution, which amounts to an initial length of ~100 μm and a volume of ~0.4 nL. These results are consistent with the simulations performed by Dose and Guiochon,[27] in which they predicted that 10% of a 1-mm plug penetrates into the column in the first 2 s after presentation of a sample that has a slightly higher diffusion coefficient than that of fluorescein. Note that in these experiments the sample solution was dissolved in the same buffer as in the filled capillary. Under these conditions, the length of injected sample upon contact with the sample never reached 700 μm, as reported previously.[9]

Penetration Kinetics in Ambient Atmosphere. In CE the capillary may not be surrounded by an environment saturated with water vapor. A similar set of penetration kinetics for capillaries held in an ambient atmosphere was quantitatively imaged using the CCD system. The experimental conditions are identical to those for the saturated environment except

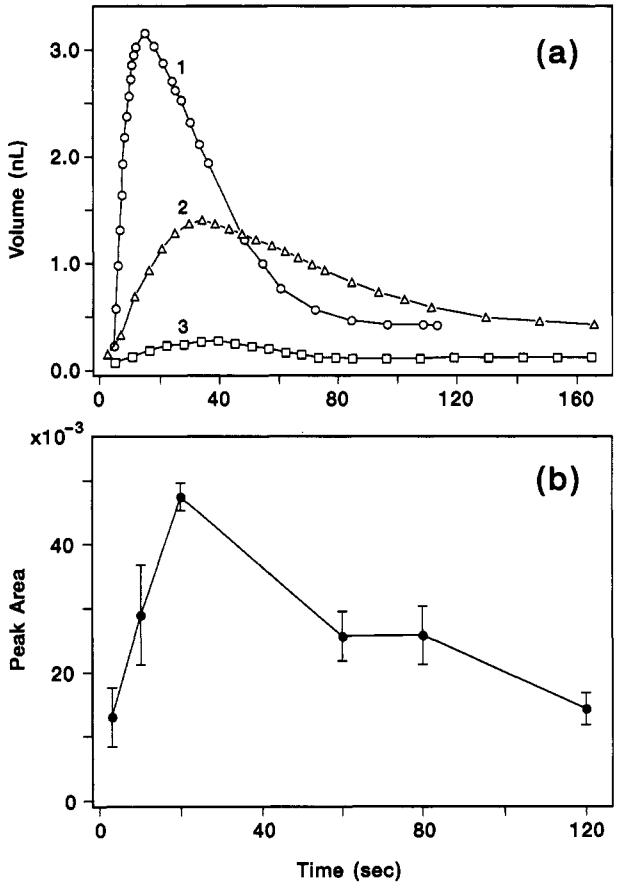

Figure 5. (a) Kinetic curves for spontaneous capillary penetration. The capillary is surrounded by an ambient environment. Each curve shows the volume of the injection plus as a function of time. Injection plugs were quantitated directly from images taken by a scientific-grade CCD camera. Shown are penetration curves for (1) 75-μm-i.d., 343-μm-o.d. capillary; (2) 50-μm-i.d., 345-μm-o.d. capillary; and (3) 25-μm-i.d., 348-μm-o.d. capillary. Statistics for the maximum injection (mean $\pm 1\sigma$): 93 $\pm$ 3 pixels (n = 3), 7.6 μm/pixel (75-μm-i.d. capillary); 68 $\pm$ 6 pixels (n = 3), 10.1 μm/pixel (50-μm-i.d. capillary); 47 $\pm$ 9 pixels (n = 3), 13.9 μm/pixel (25-μm-i.d. capillary). All other conditions the same as in Figure 3. (b) Peak area for dansylated lysine as a function of varying the transfer time. (Analysis is from electropherograms of spontaneous injection of a mixture of the three dansylated amino acids described in Figure 4.) Capillaries were surrounded by an ambient atmosphere during the transfer. Each point represents the mean peak area for a particular transfer time. Error bars represent 1σ (n = 3).

that the capillary is exposed to ambient air. Shown in Figure 5a are representative examples of penetration curves for spontaneous injection in 75-, 50-, and 25-μm-i.d. capillaries. As in the experiments with the saturated environment, a similar penetration process takes place at early times, but two significant and interesting differences are evident. First, the length of injection reaches a maximum and then becomes smaller in time. This surprising result shows that the injection plug slowly compresses into the entrace of the column, and the effect can be observed directly with video microscopy. In addition, the video images show that as the fluorescein plug retreats toward the inlet, it appears to become darker. Although direct video observation suggests that the sample is becoming concentrated in the inlet end, more rigorous experiments are needed to quantitate and elucidate the mechanism. Second, the maximum length of injection at the peak is lower than it is in a saturated atmosphere. A likely explanation is that the droplet volume is being reduced by evaporation during the injection.

Several different control experiments suggest that evaporation of the buffer is what affects the injection length. By positioning sample solution at different distances from the inlet of the capillary after injection, the effective vapor pressure surrounding the capillary and droplet is made to vary. At distances very close to the inlet, the vapor pressure is high and falls off as the distance is increased. We find that the amount of injected volume increases when the capillary is closer to the surface of the sample solution after injection. Moreover, under these conditions, the degree the sample is compressed is minimized. Thus by holding the capillary directly above the solution, we could obtain penetration curves similar to those in the vapor-saturated chamber. In addition, if evaporation were occurring, a presure difference would be created, and consequently, the outlet buffer would be drawn into the capillary. To test this idea, the outlet capillary end was imaged during the delay time. When the inlet end was held in ambient conditions, fluorescein in the outlet vial entered and filled the entire end of the imaged part of the capillary. The same test was performed with the inlet held in a saturated chamber. Only a negligible amount of the fluorescein was observed to enter, as expected by diffusion.

Figure 5b illustrates the effect of differential delay time on peak area when the capillary is held in an ambient atmosphere. Again, each point is the average peak area that results from a separation of dansylated lysine resulting from a different transfer time. As was evidenced by direct CCD imaging, the trend in the peak area shows that the injection volume grows in size, reaches a maximum, and then decreases as a function of delay time. Similarly, Figure 6 shows a series of electropherograms of three dansylated amino acids, each differing only in the delay time between withdrawing the capillary and reinserting it into the inlet buffer reservoir. A similar trend in peak height is apparent.

To summarize the results, Figure 7 directly compares spontaneous injection between saturated and ambient conditions and between CCD imaging and peak area analysis. Figure 7a compares the length of injection (converted to a volume) meaured with the CCD, and Figure 7b compares peak areas using 50-μm-i.d., 345-μm-o.d. capillaries. These results show that variations in the vapor pressure of water surrounding the capillary can lead to injection lengths that differ by more than 1 order of magnitude if care is not taken to prevent buffer loss from the front end of the capillary. As in the saturated environment, differing transfer times also lead to errors in peak quantitation. Thus, exposure to ambient air adds an extra level of complexity to that of the two competing effects, spontaneous penetration and buffer loss (sample compression).

It is interesting that the trends in peak area are remarkably similar to the penetration curves as measured from direct CCD imaging of the plug length. If the sample were simply becoming concentrated in the end of the column, then the peak areas would increase and level off as in the experiments performed in the saturated atmosphere; furthermore, peak heights would be expected to increase at each delay time. In contrast, the decreasing peak areas and heights show that considerable sample loss occurs during some stage of the injection process under ambient conditions.

Several mechanisms for sample loss as a function of reinserting the capillary into the inlet solution have been

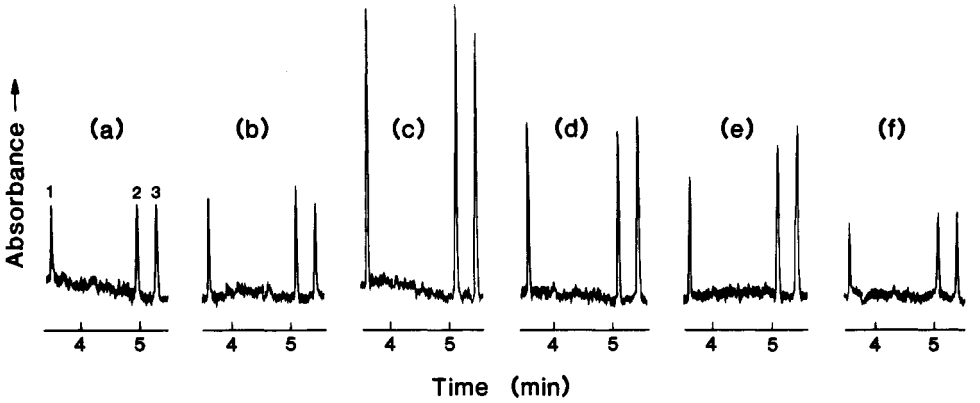

Figure 6. Effect of varying the time between transferring the capillary inlet from the sample solution and reinserting it in the inlet reservoir. The capillary was transferred in ambient atmosphere. Each electropherogram shows a separation of ~0.5 mM (1) dansyllysine, (2) dansyltryptophan, and (3) dansylalanine. The different electropherograms correspond to the following transfer times: (a) 2, (b) 10, (c) 20, (d) 60, (e) 80, and (f) 120 s. The mean and standard deviation for each set of delay times are shown in Figure 5b.

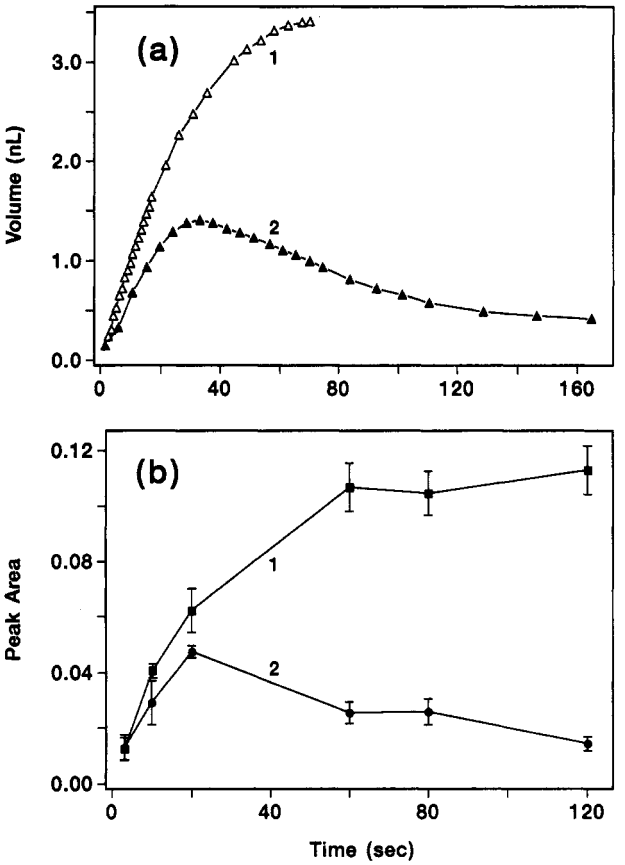

Figure 7. Comparison between spontaneous extraneous injection for delay times in (1) saturated and (2) ambient atmosphere. Shown are (a) injection lengths as determined by CCD measurements and (b) peak areas from CE separations. Both sets of curves are for a 50-μm-i.d., 345-μm-o.d. fused silica capillary. Conditions are identical to those in Figures 3–6.

thoroughly discussed by Dose and Guiochon.[27] One scenario is that as the column is reinserted into the solution, rapid outward diffusion occurs. From these results, we can predict that if the sample were actually concentrated at the entrance, then the concentration profile would be steeper in the saturated conditions, thus causing an even greater loss from the column. Another scenario is that sample simply flows out the column by inadvertent flow. Although inadvertent hydrodynamic outflow may have occurred in these experiments, it is less likely because care was taken in positioning the inlet and outlet reservoirs. Other potential mechanisms based on convective outflow[30] or Marangoni mixing[40,48] are possible, and precedence is found in the literature for them. The salient message is that when the capillary is transferred in ambient air, compression of the injection plug occurs at long delay times and loss of sample can result. This conclusion further emphasizes the need to control such factors as inadvertent hydrodynamic flow and outward diffusion by reducing the delay times between reinserting the capillary into the inlet reservoir and applying the voltage.

The consequences of the sample plug's becoming compressed into the end of the capillary are serious when longer than normal delay times occur. We have been exploring the possibility of performing chemical derivatization in the entrance of the column.[20] In some instances, the derivatization reaction is allowed to proceed for several minutes. Allowing the capillary to be exposed to air be problematic in that variable amounts of sample can be lost from the column when it is replaced in the inlet solution. Furthermore, this effect should be taken into account in experiments in which the capillary is manipulated for direct cellular sampling or for microinjection onto the column—scenarios that may require longer than usual delay times. Finally, in working with minute samples, such as single synaptic vesicles that have volumes of attoliters or less, extreme care must be taken after the sample is injected onto the column to avoid loss.

Effect of Delay Time on Gravity Injections. The magnitude of the effect of spontaneous capillary penetration on actual injections in CE depends on the length of the injection. Obviously, the volume of the extraneous injection makes up a larger fraction of a narrow zone than it does of a broader one. Figure 8 is a demonstration of the effect of spontaneous capillary penetration for two different transfer times on a 4-s gravity injection during which the sample is elevated 3.8 cm above the outlet. The capillary is held directly above the sample droplet so that it is in a nearly saturated environment. The peaks shown are representative of several runs for each delay time. The average peak area increases by a factor of 2 when the delay time changes from 1 to 10 s. Such a variation in peak area would lead to poor quantitative accuracy and precison. A typical injection penetration curve (Figure 3) shows fast kinetics in the initial portion of the curve and slower penetration velocities as the curve levels off. If the delay time

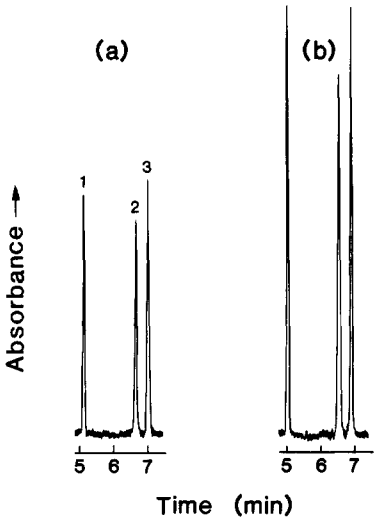

Figure 8. Effect of spontaneous capillary displacement on a 4-s gravity injection. The sample is held 3.8 cm above the outlet solution. Shown are electropherograms of ~0.5 mM (1) dansyllysine, (2) dansyltryptophan, and (3) dansylalanine that differ only in the transfer time between injecting the sample and reinserting the capillary in the inlet reservoir. Transfer times are (a) 1 s and (b) 10 s. Several runs were performed, and the electropherogram shown is representative of the mean peak area for the dansylated lysine peak. Peak area statistics (mean $\pm 1\sigma$): 0.29 ± 0.01 (n = 3), 1-s transfer delay; 0.15 ± 0.02 (n = 3), 10-s transfer delay. Separation capillary, 75-μm i.d. × 62 cm (27 cm to detector); buffer, 15 mM phosphate, pH 8.9; 16kV voltage.

is increased such that it merely extends further into the slow portion of the penetration curve, only a minimal additional contribution from spontaneous fluid displacement on the gravity injection results. When a similar experiment is performed under ambient conditions, however, investigation by CCD imaging and peak area analysis reveals that long delay times (>60 s) result in a significant reduction in injection length and loss in peak area. For shorter delay times (<20 s), a variation in peak area analogous to that found under saturated conditions is predicted from findings shown in Figures 5 and 6. Results from gravity injections carried out in both saturated and ambient environments suggest that reproducibility for small injections can be improved by maintaining constant delay time after each injection.

Minimizing Spontaneous Injection. Our results indicate that a main contribution to the extraneous injection in 75-, 50-, and 25-μm-i.d., ~345-μm-o.d. capillaries is from spontaneous fluid displacement. Consequently, several approaches for dramatically minimizing this extraneous injection are now possible. Minimizing the volume of the droplet, lowering the interfacial pressure difference by decreasing the curved surface, or providing a counteracting back pressure all act to decrease penetration. As indicated in eq 5, when the outlet reservoir is raised above the inlet reservoir, a back pressure, ρgh, from the gravitational weight of the water results in slowing the penetration process. In fact, we found that by raising the outlet by 18 cm, no detectable injection was observed, either during initial contact or after the capillary was removed from the sample. In addition, we found that introducing a 1-cm height difference minimized penetration of sample during the initial contact. This result is in contrast to previous findings[9] that even in the presence of a 5-cm height difference, significant injection occurred upon initial contact with the sample.

Another approach is to reduce the droplet volume by reducing the outer diameter of the capillary. Because the droplet spans entirely across the end surface of the capillary, the size of the droplet is defined by the morphology (and size) of the outer diameter of the capillary. Any reductions in the outer diameter will significantly minimize the size of the droplet that forms. Figure 9 illustrates the effect of etching the outer diameter of the capillary to ~110–120 μm with hydrofluoric acid. These video images show a reduction in the amount of sample penetration after the etched capillary is removed from the solution. The slightly jagged end of the etched capillary may have helped in reducing the effective surface for droplet attachment. As evidenced, most of the injection occurred during the initial contact. Representative separations comparing untreated and etched capillaries are shown in Figure 10. A reduction in the amount of spontaneous extraneous injection by as much as ~12-fold can be achieved by etching the capillary. In each set of runs, the time delay before the etched capillary is reinserted into the inlet vial is 10 s. By minimizing the formation of a curved meniscus at the inlet end of the capillary, there should be comparatively no dependence on the delay time. Indeed, Figure 11 shows little difference in amount injected by changing the delay from 2 to 10 s for an etched capillary. Alternatively, to show that a reduction in injection length can be achieved with a smoother, less jagged surface, we tested well-cleaved, thin-walled capillaries that maintain the same inner diameter but have smaller outer diameters. From video and CCD imaging data, a reduction by ~7-fold in the length of spontaneous injection was found with commercially available thin-walled capillaries (131-μm o.d., 52-μm i.d.). These data suggest that the use of etched capillaries or thin-walled capillaries will improve reproducibility and separation efficiencies.

As discussed earlier, methods that change the wettability of the surface can also affect the degree of extraneous penetration by affecting the volume of the droplet reservoir that adheres to the end surface. One approach is to make the outside surface of the capillary more hydrophobic, which makes it more difficult for the solution to wet to the surface and can reduce the droplet size. Some silanized capillaries did result in a slight reduction of peak areas (~2-fold) for the spontaneous injection, and this conclusion was qualitatively confirmed by observing a smaller droplet at the end of the capillary with video imaging. We found it difficult, however, to make reproducible reduced droplet volumes with the silanization procedure used in these studies. The other possibility is to lower the apparent contact angle by adding surfactant to the sample, which has the effect of increasing surface wetting by inducing greater spreading onto the sides of the capillaries, as described by Adamson.[40] Again, the reservoir volume is reduced but from a different mechanism, that of the droplet spreading onto the outside surface of the capillary. As an example, we found spreading to occur when sodium dodecyl sulfate (SDS) (Life Technologies Inc., Gaithersburg, MD) was added to the sample (solution was 50% in SDS). In general, it is important to understand the surface wettability with respect to both the sample and buffer solution for controlling spontaneous injection.

(49) Ruckenstein, E.; Suciu, D. G.; Smigelschi, O. In *Modern Approaches to Wettability: Theory and Applications*; Schrader, M. E., Loeb, G., Eds.; Plenum: New York, 1992; pp 379–422.

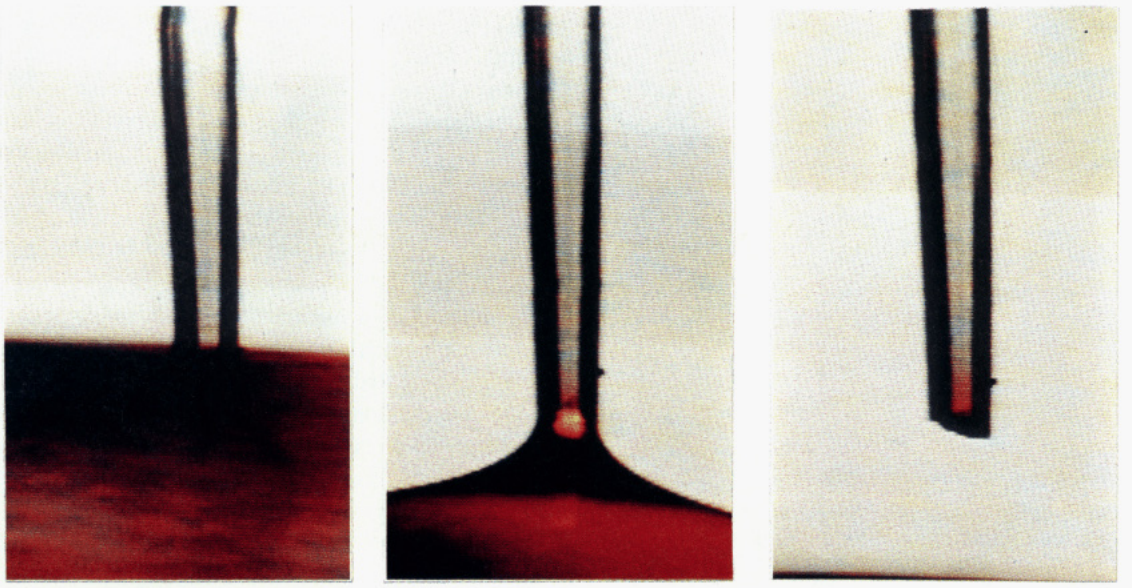

Figure 9. Video images showing the inlet end of a 75-μm-i.d., 343-μm-o.d. capillary that has been etched down to ~130-μm o.d. with hydrofluoric acid (0.1 M) and then silanated: (a) insertion into solution, (b) contact with sample immediately before solution breakage, and (c) ~10 s after leaving solution.

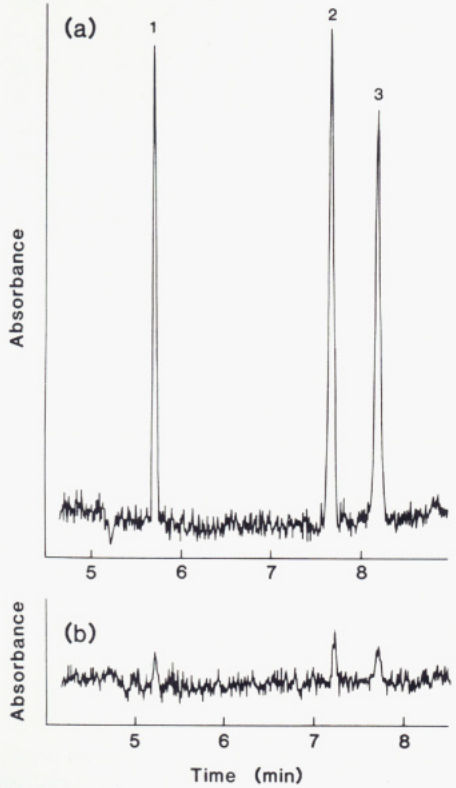

Figure 10. Electropherogram comparing spontaneous extraneous injection in an (a) untreated and (b) etched capillary. Separation of ~0.5 mM (1) dansyllysine, (2) dansyltryptophan, and (3) dansylalanine. Separation capillary, 75 μm i.d. × 62 cm (27 cm to detector); buffer, 15 mM phosphate, pH 8.9.

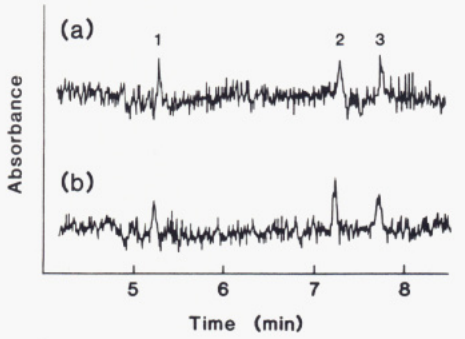

Figure 11. Comparison of different delay times between injection and reinsertion into the inlet vial for etched column: (a) 2- and (b) 10-s delay before reinsertion. All conditions are the same as in Figure 10.

CONCLUSION

We have identified that spontaneous fluid displacement resulting from an interfacial pressure difference is a main cause for extraneous injection in 25-, 50-, and 75-μm-i.d., ~345-μm-o.d. fused silica capillaries. By characterizing this mechanism, we have discovered new parameters that must be controlled to achieve small injections in a quantitative manner. These parameters include precise timing between withdrawing the capillary from the sample and reinserting it into the inlet reservoir, constant vapor pressure surrounding the capillary during the transfer time, and reproducible surface wettability and morphology of the capillary walls at the inlet. Consideration of these results is essential when claims are made for high-sensitivity mass analysis, particularly in 360-μm-o.d. and larger capillaries. Extreme care must be taken with long delay times to prevent significant loss of buffer from the end of the column and compression of the sample. Because this effect can lead to sample losses, it is important to consider for applications such as on-column derivatization[20] and single-cell analysis. Finally, we have developed several methods to minimize spontaneous injection including etching the outer diameter of the capillary inlet, using a thin-walled capillary, and manipulating the wettability of the surface at the inlet. Whichever strategy is implemented, the reduction in the extraneous injection should lead to better separation efficiency and to more precise quantitation for ultramicrosampling in capillary electrophoresis.

ACKNOWLEDGMENT

We thank Professor George M. Homsy of the Stanford University Chemical Engineering Department and Professor Jonathan V. Sweedler of the University of Illinois Chemistry Department for many useful discussions and advice. We are also grateful to Rajeev Dadoo, Jason B. Shear, and Robert Guettler for many helpful comments on the manuscript. H.A.F. is a W. R. Grace Fellow. This work was supported by Beckman Instruments, Inc. and the National Institutes of Mental Health (Grant NIH 5RO1 MH45423-03).

Received for review December 21, 1993. Accepted March 25, 1994.•

• Abstract published in *Advance ACS Abstracts,* May 15, 1994.